Carbohydrate Polymers 76 (2009) 51–59

Contents lists available at ScienceDirect

Carbohydrate Polymers

journal homepage: www.elsevier.com/locate/carbpol

Cellulose microfibrils from banana rachis: Effect of alkaline treatments on structural and morphological features

Robin Zuluaga [a,b,1], Jean Luc Putaux [c,2], Javier Cruz [a], Juan Vélez [d], Iñaki Mondragon [e], Piedad Gañán [a,*]

[a] School of Engineering, Mechanical Engineering Program, New Materials Research Group, Pontificia Bolivariana University, Circular 1 # 70-01, Medellín, Colombia
[b] School of Engineering, Agro-Industrial Engineering Program, New Materials Research Group, Pontificia Bolivariana University, Circular 1 # 70-01, Medellín, Colombia
[c] Centre de Recherches sur les Macromolécules Végétales (CERMAV-CNRS), BP 53, F-38041 Grenoble cedex 9, France
[d] Science and Engineering Materials Group, National University of Colombia, Carrera 80, # 65-223, Medellín, Colombia
[e] "Materials+Technologies" Group, Chemical and Environmental Engineering Department, Polytechnic School, Universidad del País Vasco/Euskal Herriko Unibertsitatea, Pza. Europa, 1. 20018. Donostia - San Sebastián, Spain

ARTICLE INFO

Article history:
Received 13 August 2008
Received in revised form 12 September 2008
Accepted 18 September 2008
Available online 30 September 2008

Keywords:
Banana rachis
Agro-industrial residues
Cellulose microfibrils
Chemical treatments
Crystalline structure

ABSTRACT

Four different alkaline treatments for isolation of cellulose microfibrils from vascular bundles of banana rachis were comparatively studied. Isolated cellulose microfibrils were characterized using high performance anion exchange chromatography for neutral sugar composition, as well as attenuated total reflection Fourier transform infrared spectroscopy, transmission electron microscopy, X-ray and electron diffraction and solid-state ^{13}C NMR. The cellulose microfibrils treated with peroxide alkaline, peroxide alkaline–hydrochloric acid or 5 wt% potassium hydroxide had average diameters of 3–5 nm, estimated lengths of several micrometers. Although the interpretation of their structure is difficult because of the low cristallinity, X-ray diffraction, ^{13}C NMR and ATR-FTIR results suggested that cellulose microfibrils from banana rachis could be either interpreted as cellulose IV_1 or cellulose Iβ. The specimens treated with a more concentrated KOH solution (18 wt%) were still microfibrillated but their structure was converted to cellulose II.

1. Introduction

Banana plant farming is one of the main agro-industries in Colombia. This activity generates a considerable amount of fibrous residues as rachis. This residue is the bunch axis in the plant that is cut after harvesting and usually left in the soil plantation. However, the vascular bundles of this material have received attention as new reinforcing agents in the elaboration of composite materials (Faria, Cordeiro, Belgacem, & Dufresne, 2006) or for the isolation of cellulose microfibrils (Zuluaga, Putaux, Restrepo, Mondragon, & Gañán, 2007).

Cellulose, the most common organic substance in nature, is the main structural component that confers strength and stability to the plant cell walls (Dufresne, 2006). It is found in the cell walls as a network of microfibrils embedded in a non-cellulosic matrix (Rondeau-Mouro et al., 2003).

Several processes are used to extract highly-purified microfibrils from the cell wall. They are generally based on successive chemical and mechanical treatments. Chemical treatments with alkaline solutions at different concentrations were used to isolate microfibrils from sugar beet (Dinand, Chanzy, & Vignon 1999; Dufresne, Cavaillé, & Vignon, 1997), potato tuber cells (Dufresne, Dupeyre, & Vignon, 2000) both cladodes and spines from *Opuntia ficus-indica* (Malainine et al., 2003), prickly pear fruits of *O. ficus-indica* (Habibi, Heux, Mahrouz, & Vignon, 2008), lemon and maize (Rondeau-Mouro et al., 2003), soybean (Wang & Sain, 2007), sisal (Morán, Alvarez, Cyras, & Vázquez, 2008) and hemp fiber (Wang, Sain, & Oksman, 2007). These treatments led to partial separation of the microfibrils from the cell wall, taking advantage of its relatively low lignin and hemicellulose content. However, none of these works analyzed the influence of several alkaline solutions at different concentrations on the structure and morphology of isolated cellulose microfibrils. In addition, to improve the individualization of the microfibrils, several mechanical treatments such as cryocrushing (Chakraborty, Sain, & Kortschot, 2005) and Manton-Gaulin homogenizing (Dufresne et al., 1997; Turbak, Snyder, & Sandberg, 1983) have been used, yielding highly viscous suspensions of individual cellulose microfibrils. Another mechanical route consists in homogenizing cellulose using a Waring Blender equipment after

* Corresponding author. Tel.: +57 4 4159095; fax: +57 4 4112372.
E-mail addresses: robin.zuluaga@upb.edu.co (R. Zuluaga), piedad.ganan@upb.edu.co (P. Gañán).
[1] Tel.: +57 4 4159095; fax: +57 4 4112372.
[2] Affiliated with Université Joseph Fourier and member of the Institut de Chimie Moléculaire de Grenoble.

0144-8617/$ - see front matter Crown Copyright © 2008 Published by Elsevier Ltd. All rights reserved.
doi:10.1016/j.carbpol.2008.09.024

oxidation mediated by the 2,2′,6,6′-tetramethylpiperidine-1-oxyl (TEMPO) radical (Saito, Nishiyama, Putaux, Vignon, & Isogai, 2006).

In order to investigate the potential of cellulose microfibrils isolated from vascular bundles of banana rachis as reinforcement in biocomposite applications (Azizi Samir, Alloin, & Dufresne, 2005; Hubbe, Rojas, Lucia, & Sain, 2008; Yano & Nakahara, 2004), this study was focused on the effect of different chemical treatments on microfibrils structure. Chemical modifications in the samples after the various extraction and purification treatments were analyzed using high performance anion exchange chromatography with pulsed amperometric detection (HPAEC-PAD) and attenuated total reflection Fourier transform infrared spectroscopy (ATR-FTIR). Morphological analysis of isolated microfibrils was performed by transmission electron microscopy (TEM). In addition, X-ray diffraction (XRD) was used to follow the fibrous transformation of native cellulose I into cellulose II. Finally, solid-state ^{13}C NMR was used to monitor the structural changes that took place in the samples depending on the extraction treatments.

2. Experimental

2.1. Materials

Banana rachises were obtained from the Uraba region in Colombia. First, they were washed with distilled water for 10 min, followed by an extraction either by biological retting (Gañán, Cruz, Garbizu, Arbelaiz, & Mondragon, 2004a; Gañán, Zuluaga, Vélez, & Mondragon, 2004b) or by mechanical processing (Tilby, 1994), in order to isolate the vascular bundles. The vascular bundles were cleaned with fresh water and dried at 90 °C overnight. For microfibril isolation, the vascular bundles were cut into 100–300 mm pieces, and these chunks were ground to pass a 2.0 mm size sieve. The chemical composition of vascular bundles is 48.7 wt% cellulose, 16.1 wt% hemicelluloses, 12.2 wt% lignin and 7.9 wt% ash on a dry weight basis.

2.2. Isolation of cellulose microfibrils

Cellulose microfibrils were prepared using different combinations of chemical and mechanical treatments. The treatments and codifications of the samples are summarized in Fig. 1 and described in the following. The main objective of these treatments was to eliminate non-cellulosic components such as pectic substances, hemicelluloses and lignin.

The samples labeled PA and PA–HCl were treated with 0.5 M NaOH solution (300 mL) under mechanical stirring at 30 °C for 18 h. Then, the insoluble residue was treated with 0.5 M NaOH and 3 wt% H_2O_2 solution (200 mL) at 45 °C for 14 h. For the sample labeled PA, a second treatment with 2 M NaOH solution (200 mL) at 55 °C for 2 h was used, whereas in order to remove mineral traces in the sample named PA–HCl, the step with 2 M NaOH was replaced by 2 M HCl (200 mL) at 80 °C for 2 h (Dinand et al., 1999).

To prepare the sample labeled KOH-5, a 5 wt% KOH solution (300 mL) was vigorously stirred at room temperature for 14 h. Then, the insoluble residue was delignified with 1 wt% $NaClO_2$ (200 mL) at pH 5.0, and adjusted with 10 wt% acetic acid, at 70 °C for 1 h. A second treatment with KOH solution (200 mL) under the same conditions as in the first step was used. Finally, a 1 wt% HCl solution (200 mL) at 80 °C for 2 h was added to remove mineral traces. For samples labeled KOH-18, the concentration of KOH was increased from 5 to 18 wt% but the same conditions of time, temperature and volume were used.

At each step of the different treatments, the insoluble residue was extensively washed with distilled water for several hours, until pH was neutral. All samples were homogenized in a Waring blender for 10 min at a concentration between 3 and 4 wt%.

2.3. Scanning electron microscopy (SEM)

SEM was used to investigate the microstructure and the surface morphology of vascular bundles of banana rachis. Samples were embedded in paraffin wax and air-dried overnight. Transverse sections were cut using a rotary microtome. Thicker sections were coated with gold/palladium using an ion sputter coater and observed with a Jeol JSM 5910 LV microscope operated at 15 kV.

2.4. Neutral sugar composition

Samples were hydrolyzed by adding approximately 50 mg of the material to 0.5 mL of 72 wt% sulfuric acid. The mixture was

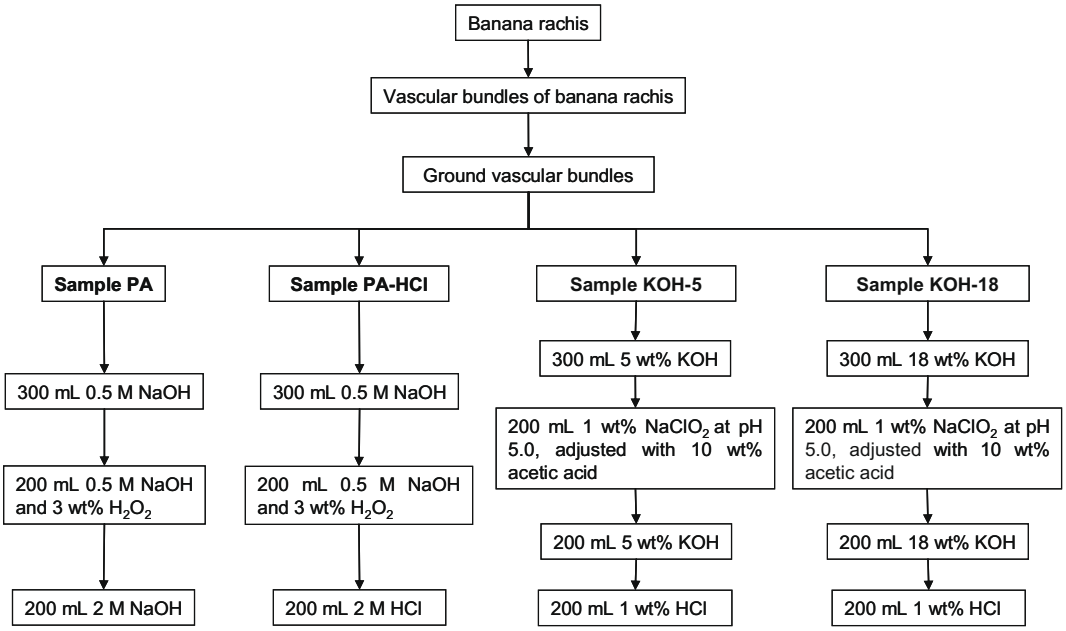

Fig. 1. Scheme for isolation of cellulose microfibrils from vascular bundles of banana rachis by four different chemical treatments.

heated in a water bath at 30 °C for 1 h and then diluted to 4 wt% sulfuric acid concentration with deionized water. The diluted mixture was then heated at 105 °C for 150 min in closed tubes, before ice cooling.

An analysis of monosaccharides on the hydrolyzed sample was performed using high performance anion exchange chromatography with pulsed amperometric detection (HPAEC-PAD). The equipment consisted of a Dionex GP50 gradient pump, ED50 electrochemical detector, AS50 autosampler and a Carbopac™ PA1 column. Samples injected into the system were eluted with 0.004 M NaOH (carbonate-free and purged with helium) with post-column addition of 0.3 M NaOH at a rate of 1 mL/min. Run time was 45 min, followed by 8 min elution with 0.5 M NaOH solution to wash the column and then 15 min elution with 0.004 M NaOH solution to re-equilibrate the column. The analysis was quantified against three separated standard solutions using the Chromeleon™ computer software. The quantified monosaccharides were arabinose, rhamnose, glucose, xylose and mannose. The monosaccharide purity of the isolated samples was determined as the percentage composition of the quantified monosaccharides based on a weight/weight ratio.

2.5. Attenuated total reflection Fourier transform infrared spectroscopy

Infrared spectroscopy experiments were conducted using a FTIR spectrometer (Nicolet 6700 Series) equipped with a single-reflection ATR and a type IIA diamond crystal mounted in tungsten carbide. The diamond ATR had approximately 0.5 mm^2 sampling area, where a consistent reproducible pressure was applied to every sample. Infrared spectra were collected at 4 cm^{-1} resolution and 256 scans were carried out.

2.6. Transmission electron microscopy

The samples obtained after chemical and mechanical treatments were diluted using distilled water and sonicated to achieve a good dispersion. Drops of each suspension were deposited onto glow-discharged carbon-coated electron microscope grids and negatively stained with 2 wt% uranyl acetate. Unstained specimens were also prepared for electron diffraction and observed under low illumination at low temperature (−180 °C). All samples were analyzed using a Philips CM200 'Cryo' microscope operating at an acceleration voltage of 80 kV for imaging and 200 kV for diffraction. Images were recorded on Kodak SO163 films and diffraction patterns on Fujifilm imaging plates, read using a Fujifilm BAS 1800 II bio-imaging analyzer.

2.7. X-ray diffraction

Cellulose microfibrils suspensions were centrifuged at 13,400 rpm and the pellets were allowed to dry on a teflon surface. The resulting films were X-rayed using a Philips PW3830 generator operating at the Ni-filtered CuKα_1 radiation wavelength (λ = 1.542 Å). Powder diffraction patterns were recorded on Fujifilm imaging plates and read using a Fujifilm BAS 1800 II bio-imaging analyzer.

Diffraction profiles were obtained by radially integrating the intensity of the powder diffraction diagrams. The diffraction peaks were fitted using pseudo-Voigt functions.

2.8. CP/MAS ^{13}C nuclear magnetic resonance

Solid-state ^{13}C NMR spectra were recorded on a Bruker AV-400-WB spectrometer with a triple probe channel of 4 mm, with rotors of ZrO and a stopper of Kel-F at room temperature. The speed of rotation was 8 kHz and the pulse sequence employed was cross-polarization (CP-MAS) ^{1}H ^{13}C, using a spectral width of 35 kHz, a contact time of 3 ms and a relaxation time of 4 s with decoupling ^{1}H. The scan amount was 2048. The chemical shift was established in relative ppm to tetramethylsilane (TMS) as primary reference and the signal of adamantine CH_2 (29.5 ppm) was used as secondary reference. The deconvolution in C1 region in all spectra was performed by assigning Lorentzian line shapes.

3. Results and discussion

SEM micrographs in Fig. 2 illustrate the architecture of the cross-section area of vascular bundles isolated from banana rachis. As observed in other natural fibers (Engels & Jungs, 1998; Gritsch, Kleist, & Murphy, 2004; Satyanarayana, Pillai, Sukumaran, Rohatgi, & Vijayan, 1982; Zhong, Burk, & Ye, 2001), they are constituted by elementary fibers (Fig. 2a). As previously reported, each elementary fiber consists of helical spirals, namely the macrofibrils (*mf*). As shown in Fig. 2b, a thick cell wall (*cw*), generally containing non-cellulosic polysaccharides, is observed. This cell wall has a width ranging from 1 to 2 μm (Gañán et al., 2008). Also in Fig. 2b, the middle lamella (*ml*), largely consisting of pectinaceous substances, can be seen. It can be recognized as a thin layer between two adjacent elementary fibers (Dickinson, 2000).

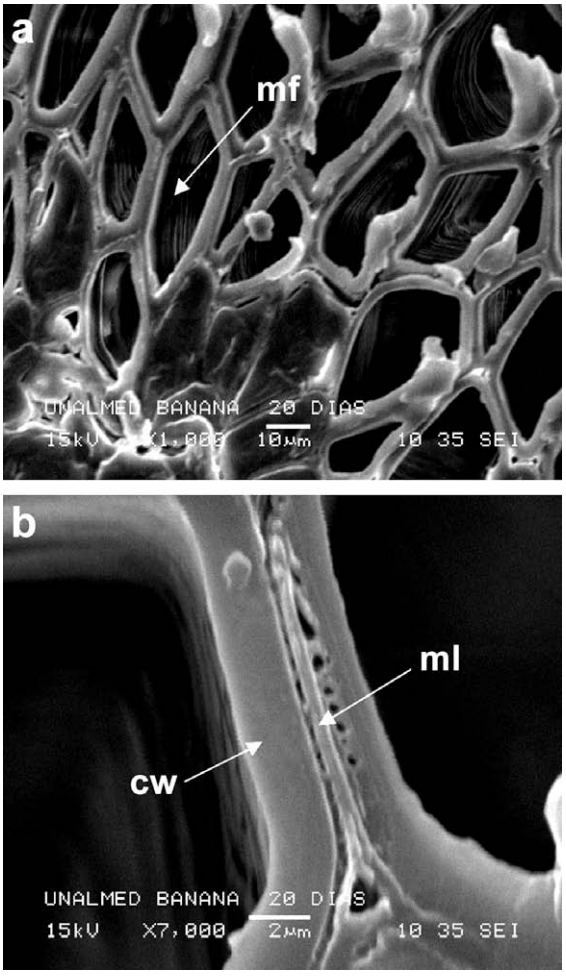

Fig. 2. (a) SEM micrograph of the vascular bundles in banana rachis and (b) micrograph at higher magnification. *mf*, macrofibrils; *cw*, cell wall; *ml*, middle lamella.

The individualization of cellulose microfibrils from banana resources was based on protocols combining chemical and mechanical treatments. During chemical treatments, constituents like pectins and hemicelluloses were hydrolyzed by the action of alkaline solutions, whereas lignin was removed during additional steps using sodium chloride or hydrogen peroxide (Fig. 1). To improve and achieve an acceptable dispersion level in the solution, mechanical homogenization with a Waring blender was also used for all samples.

The monosaccharide composition of vascular bundles and isolated cellulose microfibrils is reported in Table 1. With exception of PA treatment, these results indicate that sequential extractions contributed to remove quite well arabinose and rhamnose. Analysis by HPAEC-PAD after hydrolysis of the samples using sulfuric acid revealed that glucose was the predominant monosaccharide. Noticeable amounts of non-cellulosic sugars as xylose and mannose were also detected. The resistance to extraction with alkali of these sugars that are the main constituents of hemicelluloses is due to the association between xyloglucan and cellulose that is very strong. Xyloglucan probably binds not only to the surface of cellulose microfibrils, but it can also be entrapped within the microfibrils (Habibi et al., 2008; Kacuráková, Capek, Sasinková, Wellner, & Ebringerová, 2000; Liu et al., 2006). Xylans, xyloglucans, and glucomannans are all able to bind onto cellulose fibrils in a manner similar to the interchain bonding of cellulose itself (Renard & Jarvis, 1999). As can be seen in Table 1, KOH-18 samples exhibited minor quantities of xylose, thus indicating that removal of xylose increased with a higher concentration of KOH. These results are in agreement with the work by Hayashi, Marsden, and Delmer (1987). These authors reported that concentrated alkali solutions were effective to dissolve xyloglucan from the macromolecular complex of etiolated pea stem. This is because concentrated solutions, which cause microfibril swelling, allow the extraction of xyloglucan; with mild alkali the complex between xyloglucan and cellulose could not be broken.

FTIR spectroscopy is an appropriate technique to establish the variations introduced by different treatments on the chemical structure of the isolated samples. Fig. 3a shows ATR-FTIR spectra of the vascular bundles and isolated cellulose microfibrils after alkaline treatments. The broadened band of the OH-stretching at around 3650–3000 cm^{-1} is observed in all spectra. The two small bands at 3487 and 3442 cm^{-1} in KOH-18 samples (Fig. 3b) have been assigned to intramolecular hydrogen bonding in cellulose II (Sao, Mathew, & Ray, 1987). The vibration at 2850 cm^{-1} originating from C—H stretching in lignin and waxes was eliminated after the different chemical treatments (Gañán et al., 2004a; Gañán et al., 2004b; Xu et al, 2007a; Xu et al, 2007b). The shoulder at 1732 cm^{-1}, that represents vibrations of acetyl and uronic ester groups of hemicelluloses or ester linkage of carboxylic group of the ferulic and *p*-coumaric acids of lignin, was significantly reduced (Sun, Sung, Liu, Fowler, & Tomkinson, 2002; Sun, Xu, Sun, Fowler, & Baird, 2005). This fact indicates that the different treatments nearly cleaved this ester bond from non-cellulosic components.

Fig. 3a clearly shows that KOH-5 and KOH-18 treatments removed most of the lignin, as seen by the elimination of vibrations at 1594 cm^{-1} (aromatic ring vibrations), 1509 cm^{-1} (aromatic rings vibrations), 1460 cm^{-1} (C—H deformations) and 1235 cm^{-1} (guaiacyl ring breathing with stretching C=O), 787 cm^{-1} (C—H deformations) (Gañán et al., 2004a; Gañán et al., 2004b; Sun, Sun, Zhao, & Sun, 2004). However, the PA and PA–HCl samples showed slight changes in intensity at 1594 and 1460 cm^{-1} after treatment, suggesting that they still contained small amounts of residual lignin (Bolaños, Felizón, Heredia, Guillén, & Jiménez, 1999; Sun, Tomkinson, Mao, & Sun, 2001; Xiao, Sun, & Sun 2001; Xu, Sun, Sun, Fowler, & Baird, 2006). In particular, these vibrations were not present in KOH-5 and KOH-18 samples. This fact suggests that KOH-5 and KOH-18 treatments removed lignin more efficiently than PA and PA–HCl treatments. Sun et al. (2004) demonstrated that the method with sodium chlorite was more efficient than that with hydrogen peroxide to remove lignin.

Fig. 3b and c shows an enlargement of the 3400–3100 cm^{-1} and 1000–700 cm^{-1} regions of ATR-FTIR spectra, respectively. The absorbances at 3271 and 3241 cm^{-1} of OH stretching were not clearly evidenced, because of interfering contributions from a variety of stretching modes in the amorphous region (Liang & Marchessault, 1959). Nevertheless, the absorption band at 711 cm^{-1} assigned to Iβ cellulose was detected (Fig. 3c), meaning that the isolated cellulose microfibrils were rich in the Iβ phase (Kataoka & Kondo, 1996).The absorption band at 750 cm^{-1}, assigned to Iα, was not seen clearly in this study.

In all spectra, the band near to 1043 cm^{-1} (C—O—C stretching) is due to presence of xylans associated with hemicelluloses (Albersheim, 1976; Xu et al., 2007a; Xu et al., 2007b). This suggests that xyloglucans are strongly bound to cellulose microfibrils, as above mentioned. Interestingly, drastic change in intensity at 1102 cm^{-1} for the sample treated with 18 wt% KOH was observed (Fig. 3a). This can be associated with changes in the hydrogen bonding system (Higgins, Stewart, & Harrington, 1961; Xiao et al., 2001), and it possibly indicates the transition from cellulose I to cellulose II, as also suggested by XRD data presented below.

Results from XRD analyses are presented in Fig. 4. The diffraction patterns of PA, PA–HCl and KOH-5 samples are very similar and exhibit several broad peaks. By comparison with the spectrum of native cellulose I (using the indexation of Sugiyama, Vuong, & Chanzy 1991) the peak at the lowest angle can be described as the overlapping of $1\bar{1}0$ and 110 reflections. Then, with increasing diffraction angle, 102 and 200 and finally 004 reflections are observed. The general aspect of the spectra and, in particular, the overlapping of $1\bar{1}0$ and 110, suggest that the structure of the microfibrils corresponds to cellulose I, quite resembling cellulose IV_1, a less ordered form of cellulose I (Lai-Kee-Him et al., 2002; Wada, Heux, & Sugiyama, 2004). The XRD spectrum of sample KOH-18 is substantially different and resembles those reported for samples of viscose rayon (Hindeleh, 1980). The microfibrils thus consist of cellulose II crystallites. This spectrum displays a peak at about 12°, indexed $1\bar{1}0$, and two more intense reflections,

Table 1
Relative monosaccharide composition (wt%) in isolated cellulose microfibrils

Sugar (%)	Chemical treatments[a]				
	Vascular bundles	PA	PA–HCl	KOH-5	KOH-18
Arabinose	12.97 ± 4.49	2.75 ± 0.10	nd	nd	nd
Rhamnose	1.06 ± 0.56	nd	nd	nd	nd
Glucose	52.04 ± 2.29	73.05 ± 1.62	77.71 ± 1.11	73.91 ± 1.28	80.14 ± 0.79
Xylose	24.54 ± 5.29	16.25 ± 0.95	16.12 ± 0.97	19.11 ± 0.64	11.92 ± 0.29
Mannose	4.08 ± 1.62	7.06 ± 0.85	5.97 ± 0.39	5.85 ± 0.09	7.83 ± 0.42

nd, not detectable.
[a] Corresponding to cellulose microfibrils isolation methods described in Fig. 1.

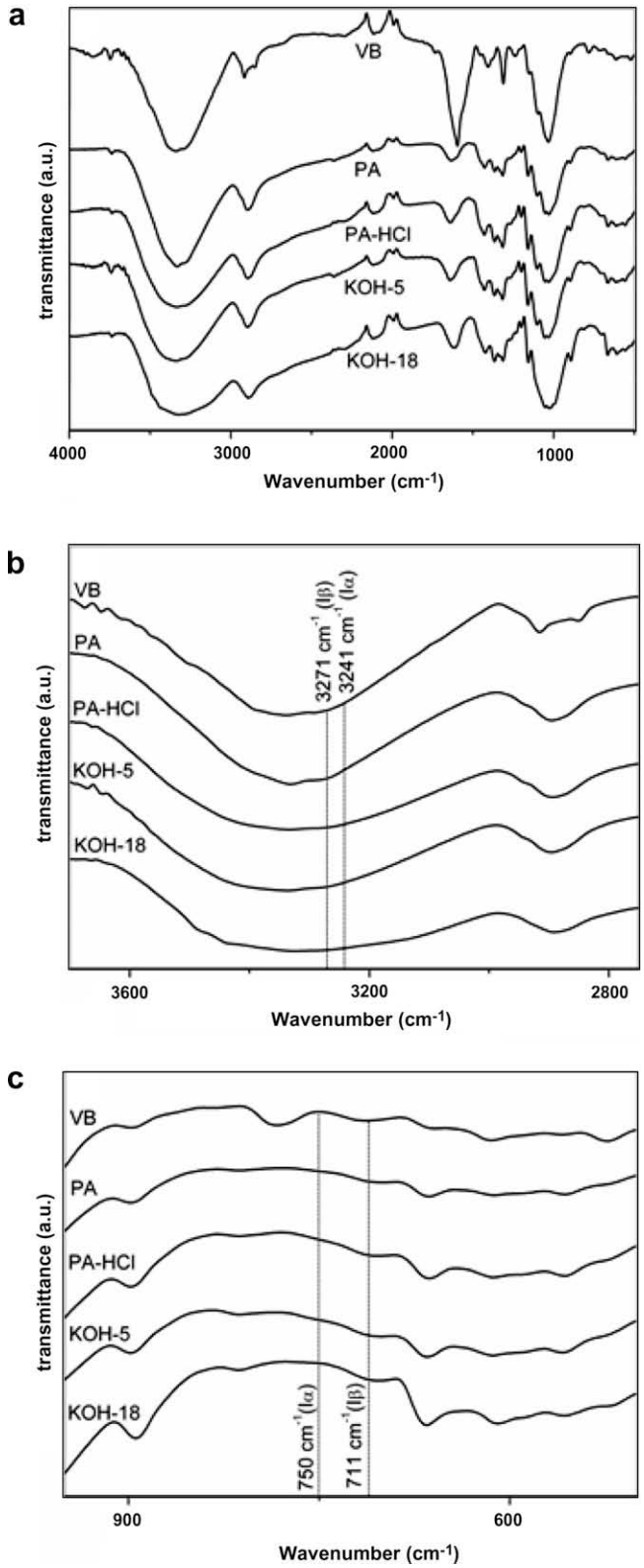

Fig. 3. FTIR spectra of isolated cellulose microfibrils after different treatments: (a) vascular bundles (VB), peroxide alkaline (PA), peroxide alkaline–hydrochloric acid (PA–HCl), potassium hydroxide 5 wt% (KOH-5) and potassium hydroxide 18 wt% (KOH-18). (b) Absorption bands at 3241 and 3271 cm^{-1} correspond to Iα and Iβ, respectively (c) Absorption bands at 750 and 711 cm^{-1} correspond to Iα and Iβ, respectively.

indexed 110 and 200. In principle, in XRD patterns recorded from perfectly isotropic cellulose II powders, these two reflections

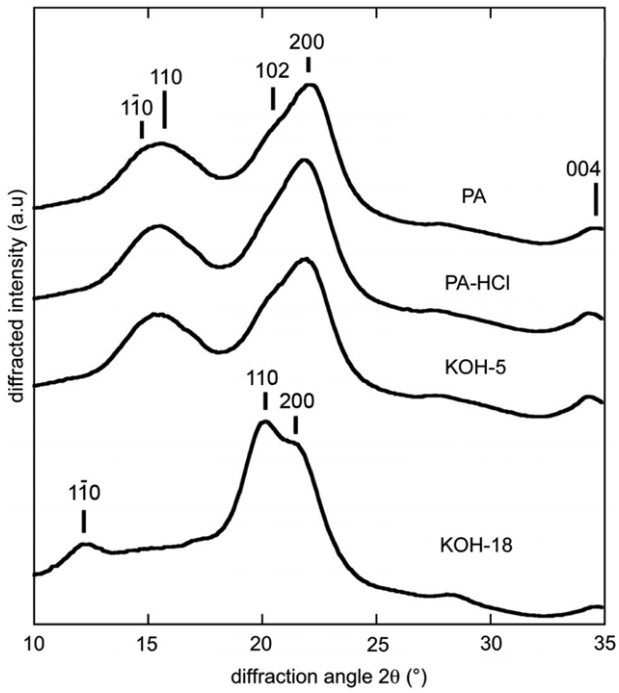

Fig. 4. X-ray diffraction spectra recorded from films of cellulose microfibrils prepared by different treatments: peroxide alkaline (PA), peroxide alkaline–hydrochloric acid (PA–HCl), potassium hydroxide 5 wt% (KOH-5), potassium hydroxide 18 wt% (KOH-18). The indexation is that defined in Sugiyama et al. (1991).

should have similar intensities. The fact that, in our spectrum, the intensity of 110 is slightly higher than that of 200 reflection may be explained by a preferential orientation of the microfibrils during the drying of the film.

As XRD spectra of samples PA–HCl and KOH-5 are very similar to that of PA-treated cellulose, we can deduce that no significant changes in crystallite size occurred during these treatments.

A comparison of the morphology of cellulose microfibrils isolated by different chemical treatments is presented in Fig. 5, where TEM micrographs recorded from negatively stained specimens are shown. The micrographs reveal that the degree of aggregation and shape of the fibrils are different. Fig. 5a (PA) and c (KOH-5) show loose networks of 40–60 nm-wide bundles of microfibrils and individual microfibrils whose diameter was estimated to be about 5 nm from enlarged TEM images. The length of the microfibrils could be estimated to a few micrometers, resulting in a practically infinite aspect ratio (Azizi Samir, Alloin, Paillet, & Dufresne, 2004). In contrast, Fig. 5b shows that PA–HCl treatment longitudinally cuts the cellulose microfibrils. This feature is typical of cellulose samples treated with strong acids that preferentially degrade the disordered regions along the microfibrils, resulting in shorter whisker-like nanocrystals (Azizi Samir et al., 2005; Lai-Kee-Him et al., 2002). Fig. 5d shows the morphology of sample corresponding to KOH-18 treatment. In contrast with other results reported in literature (Dinand, Vignon, Chanzy, & Heux, 2002), the higher KOH concentration did not result in a destruction of the cellulose microfibrils. The specimen is still microfibrillar. Several bundles are observed, and seem to contain shorter microfibrils.

Selected area of electron diffraction patterns recorded at low temperature on bundles of unstained cellulose microfibrils treated with 5 wt% and 18 wt% KOH, respectively, are shown in Fig. 6. The electron diffraction diagram recorded from sample KOH-5 can be indexed as that of cellulose I, with a strong and narrow 004 reflection on the meridional axis, and diffuse 1$\bar{1}$0, 110 and 200 reflections on the equatorial axis (Fig. 6a). In agreement with the

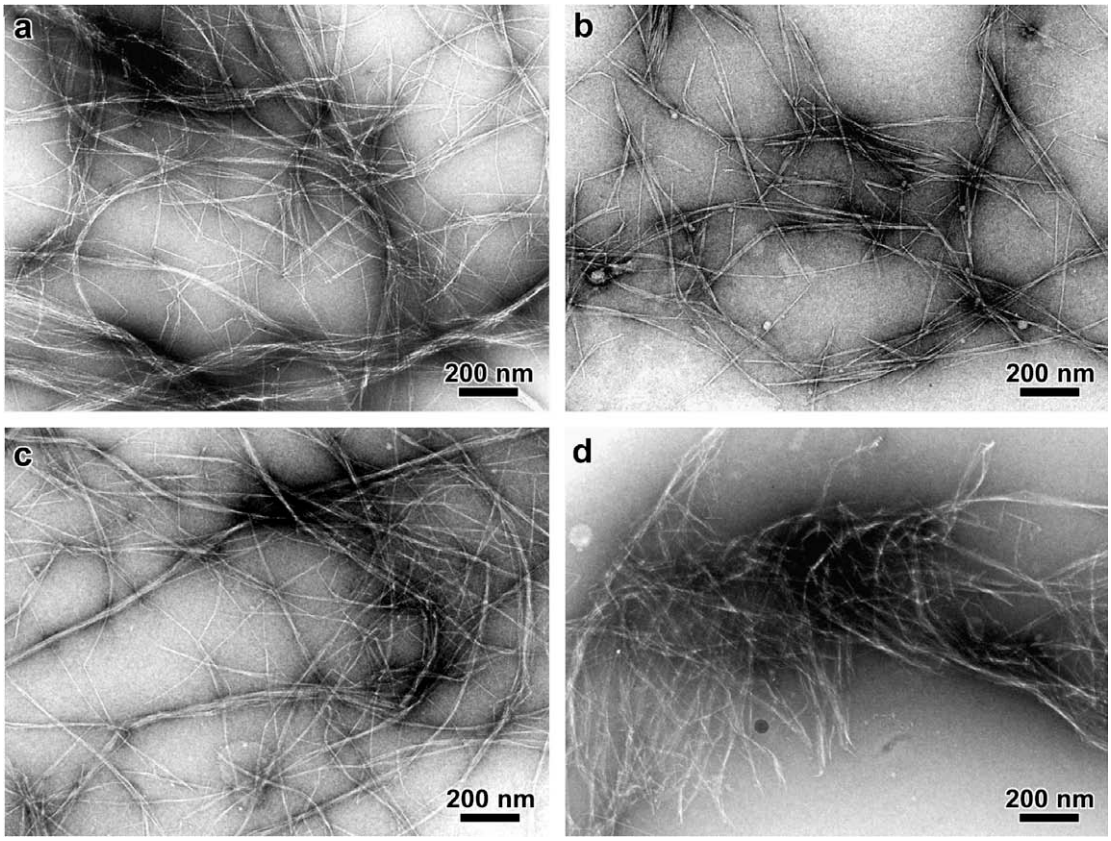

Fig. 5. TEM micrographs of negatively stained preparations of cellulose microfibrils isolated after different treatments: (a) peroxide alkaline (PA); (b) peroxide alkaline–hydrochloric acid (PA–HCl); (c) potassium hydroxide 5 wt% (KOH-5) and (d) potassium hydroxide 18 wt% (KOH-18).

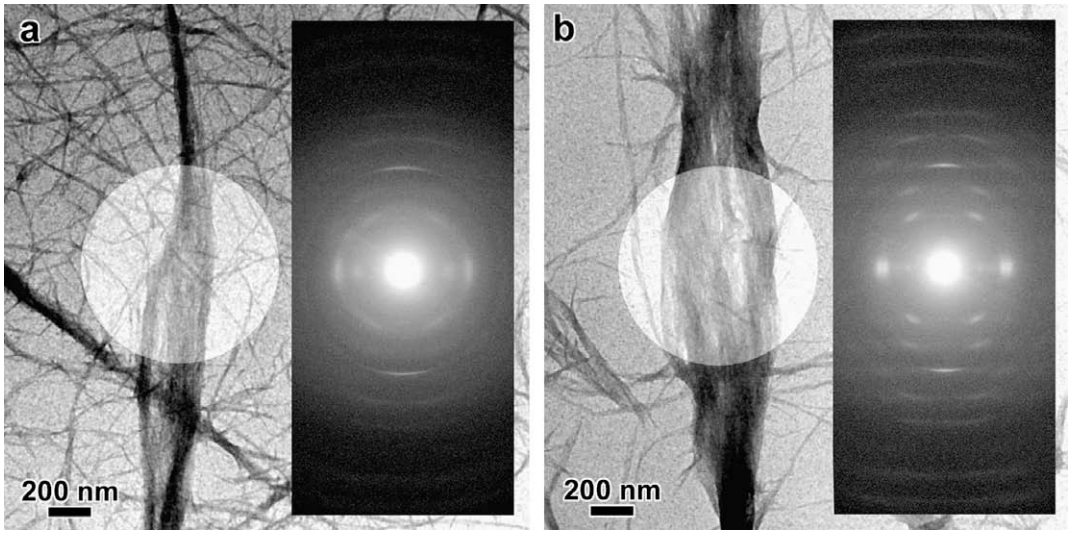

Fig. 6. TEM images of unstained bundles of cellulose microfibrils prepared using alkaline treatments KOH-5 (a) and KOH-18 (b). Inset: corresponding cellulose I and cellulose II fiber electron diffraction patterns, respectively, recorded at low temperature from the selected circular areas indicated in the image.

interpretation of the XRD spectrum of the KOH-5 sample, the fact that $1\bar{1}0$, 110 reflections are overlapping suggests that the structure is resembling that of cellulose IV_1.

Interestingly, both TEM images and X-ray/electron diffraction data concur to show that the microfibrillar nature of the KOH-18 sample was preserved while cellulose was converted to allomorph II. Other cases of fibrous mercerization of native cellulose have been reported in literature, in particular during alkaline treatments of *Valonia* (Chanzy & Roche, 1976) and ramie cellulose (Okano and Sarko; 1985; Nishiyama, Kuga, & Okano, 2000). It was shown that the parallel-to-antiparallel reorganization of cellulose chains could be initiated in the amorphous regions of alkali-swollen microfibrils. The molecules from adjacent cellulose I microfibrils with opposite chain polarity could then rearrange and crystallize into antiparallel cellulose II upon washing in water. A similar phenomenon could occur in the KOH-18 sample because the defibrillating mechanical homogenization was performed after the chemical treatments.

The ^{13}C NMR spectra of samples, PA, PA–HCl and KOH-5 (Fig. 7a) are quite similar. They are particularly broad and quite different respect to highly crystalline samples. The region between 60 and 70 ppm is assigned to C6 of the primary alcohol group. The next cluster of resonances, between 70 and 81 ppm, is attributed to C2, C3 and C5. The region between 81 and 93 ppm is associated with C4 and that between 102 and 108 ppm with C1, the carbon anomeric.

The broader C1 resonance associated to the disordered chains dominates the shape of all spectra. Nevertheless, when the C1 region is enlarged and these values are used to deconvolution with Lorentzian lineshapes (Fig. 7b), signals at 104 and 106 ppm are clearly separated, indicating that the samples are rich in cellulose Iβ (Newman, 1997), in agreement with ATR-FTIR results. In addition, the central peak at 105.4 ppm could be possibly assigned to a less ordered state and/or surface chain contributions (Wada, Okano, Sugiyama, & Horii, 1995). The resonances of cellulose occur at 89.2 ppm (core chains) and 84.8–84.2 ppm (surface chains) for C4, and 65.3 ppm (crystalline cellulose) and 63–62,9 ppm (amorphous cellulose) for the C6. The resonances of C2, C3 and C5 overlap and appear at 75.3 ppm and 72.9–72.7 ppm. It is apparent that there are no difference in supermolecular structure between the three samples. However, it is difficult to interpret these complicated ^{13}C NMR patterns; they are quite similar to pattern of cellulose IV_1 (Isogai, Usuda, Kato, Urdu, & Atalla, 1989; Wada et al., 2004).

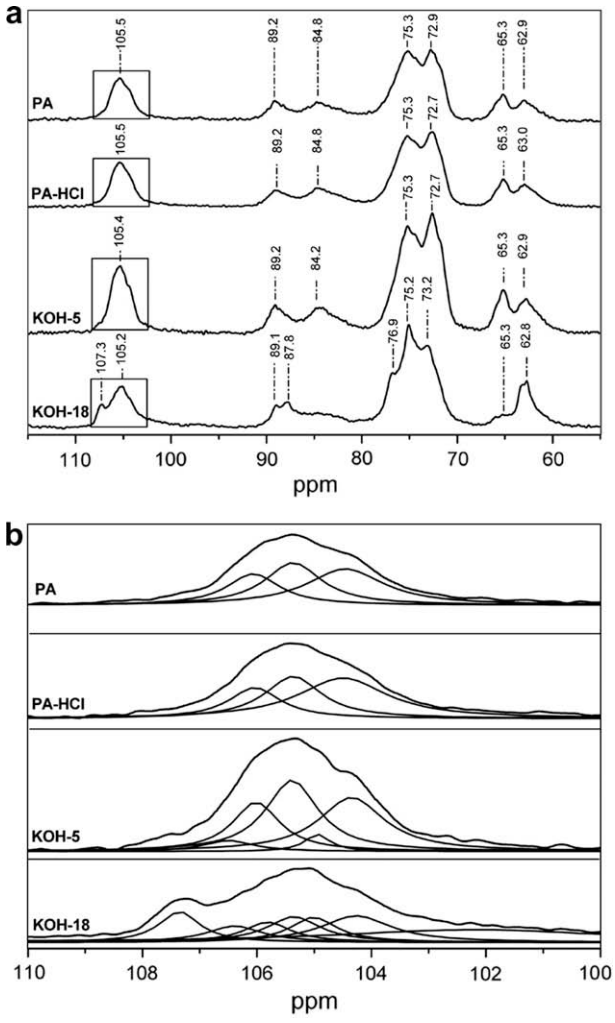

Fig. 7. Comparison of the solid-state ^{13}C NMR spectra of the isolated cellulose microfibrils after different treatments: (a) peroxide alkaline (PA), peroxide alkaline–hydrochloric acid (PA–HCl), potassium hydroxide 5 wt% (KOH-5) and potassium hydroxide 18 wt% (KOH-18); (b) enlarged C1 region of the spectra indicated by the rectangles in Fig. 7a together with the signal deconvolutions.

The ^{13}C NMR spectrum of sample KOH-18 (Fig. 7a) is typical of cellulose II, denoted by an increase in the intensity of the peak near 107.3 ppm, attributed to the C1 of the crystalline part of cellulose II (Atalla & VanderHart, 1999; Chanzy & Roche, 1976). In addition, the multiplicity of C1 resonances obtained after deconvolution arises from magnetically non-equivalent sites within crystalline domains. The transition is also identified by an increase in relative intensity of the signal at 62.8 ppm, that is associated with the amorphous regions of cellulose, and a decrease of the signal at 65.3 ppm associated with the crystalline regions of cellulose I. Both signals are assigned to C6 of the primary alcohol group (Atalla & VanderHart, 1984).

The region between 73.2 and 76.9 ppm, attributed to C2, C3 and C5, presents variations when viewed together with spectra of samples KOH-5, PA and PA–HCl. These changes may occur because of variations in hydrogen bonding patterns, as confirmed by ATR-FTIR spectra, allowing the chain adopting a new molecular conformation.

The results of diffraction, ^{13}C NMR and ATR-FTIR methods suggest that cellulose microfibrils isolated from banana rachis can correspond to cellulose IV_1, a structural form where the order of the chain direction is retained but the fibrillar sample contains crystal domains that are too narrow. Likewise, we consider that the structure is quite similar to cellulose Iβ, as reported by Helbert, Sugiyama, Ishihara, and Yamanaka (1997) in fungal cell walls and confirmed later by Wada et al. (2004) and Newman (2008).

4. Conclusions

In this work, four different treatments for cellulose microfibrils isolated from banana rachis were evaluated. By means of SEM, ion chromatography, ATR-FTIR, TEM, electron and X-ray diffraction, it was possible to study the effect of the treatment on the morphology and structure of the resulting products. ATR-FTIR confirmed the partial removal of hemicelluloses. The resistance to extraction with alkali of non-cellulosic components like xylose appears to be due to the strong association of xyloglucans and cellulose. Xyloglucans probably bind not only to the surface of microfibrils but they can also be entrapped within the microfibrils. Furthermore, the appearance in all ATR-FTIR spectra of the band near to 1043 cm^{-1} (C—O—C stretching) is undoubtedly due to the presence of xylans associated with hemicelluloses. The electron and X-ray diffraction diagrams of KOH-18 sample have revealed that microfibrillar bundles consist of cellulose II crystals, while KOH-5, PA and PA–HCl samples contain reflections associated with cellulose IV_1. The microfibrillar appearance was retained even when cellulose II was formed after strong alkali treatment. This can be related to the swelling of the initial fibers in concentrated alkali solutions, followed by chain reorganization and recrystallization during subsequent washing.

The crystallinity of the cellulose samples obtained was not high which could induce significant line broadening and difficult interpretation of ^{13}C NMR spectra. However, these patterns resemble typical patterns of cellulose IV_1. The ^{13}C NMR spectrum of sample KOH-18 is typical of cellulose II, denoted by an increase in the intensity of the peak near 107.3 ppm, attributed to the C1 of the crystalline part of cellulose II.

Results of diffraction, ^{13}C NMR and ATR-FTIR methods suggest that cellulose microfibrils isolated from banana rachis correspond to cellulose IV_1 and are quite similar to cellulose Iβ.

Acknowledgments

The authors would like to thank Colciencias for the financial support that has made this research work possible, as well as Y. Nishiyama and H. Chanzy (CERMAV) for helpful suggestions. We also thank Dr. S. Curling (Napier University) by the analyzing of monosaccharides using high performance anion exchange chromatography.

References

Albersheim, P. (1976). The primary cell wall. In J. Bonner & J. E. Varner (Eds.), *Plant biochemistry* (pp. 225–274). NY: Academic Press.

Atalla, R. H., & VanderHart, D. L. (1984). Native Cellulose: A composite of two distinct crystalline forms. *Science, 223*(4633), 283–285.

Atalla, R. H., & VanderHart, D. L. (1999). The role of solid state ^{13}C NMR spectroscopy in studies of the nature of native celluloses. *Solid State Nuclear Magnetic Resonance, 15*(1), 1–19.

Azizi Samir, M. A. S., Alloin, F., & Dufresne, A. (2005). Review of recent research into cellulosic whiskers, their properties and their application in nanocomposite field. *Biomacromolecules, 6*(2), 612–626.

Azizi Samir, M. A. S., Alloin, F., Paillet, M., & Dufresne, A. (2004). Tangling effect in fibrillated cellulose reinforced nanocomposites. *Macromolecules, 37*(11), 4313–4316.

Bolaños, F. B., Felizón, B., Heredia, A., Guillén, R., & Jiménez, A. (1999). Characterization of the lignin obtained by alkaline delignification and of the cellulose residue from steam-exploded olive stones. *Bioresource Technology, 68*(2), 121–132.

Chakraborty, A., Sain, M., & Kortschot, M. (2005). Cellulose microfibrils: A novel method of preparation using high shear refining and cryocrushing. *Holzforschung, 59*(1), 102–107.

Chanzy, H., & Roche, E. J. (1976). Fibrous transformation of Valonia cellulose I into cellulose II. *Applied Polymer Symposium, 28*, 701–711.

Dickinson, W. C. (2000). *In integrative plant anatomy*. San Diego, California: Harcourt Academic press. pp. 15–21.

Dinand, E., Chanzy, H., & Vignon, M. R. (1999). Suspensions of cellulose microfibrils from sugar beet pulp. *Food Hydrocolloids, 13*(3), 275–283.

Dinand, E., Vignon, M. R., Chanzy, H., & Heux, L. (2002). Mercerization of primary wall cellulose and its implication for the conversion of cellulose I→cellulose II. *Cellulose, 9*(1), 7–18.

Dufresne, A. (2006). Comparing the mechanical properties of high performance polymer nanocomposites from biological sources. *Journal of Nanoscience and Nanotechnology, 6*(2), 322–330.

Dufresne, A., Cavaillé, J.-Y., & Vignon, M. R. (1997). Mechanical behavior of sheets prepared from sugar beet cellulose microfibrils. *Journal of Applied Polymer Science, 64*(6), 1185–1194.

Dufresne, A., Dupeyre, D., & Vignon, M. R. (2000). Cellulose microfibrils from potato tuber cells: Processing and characterization of starch-cellulose microfibril composites. *Journal of Applied Polymer Science, 76*(14), 2080–2092.

Engels, F. M., & Jungs, H. G. (1998). Alfalfa stem tissues: Cell-wall development and lignification. *Annals of Botany, 82*(5), 561–568.

Faria, H., Cordeiro, N., Belgacem, M. N., & Dufresne, A. (2006). Dwarf Cavendish as a source of natural fibers in poly(propylene)-based composites. *Macromolecular Materials and Engineering, 291*(1), 16–26.

Gañán, P., Cruz, J., Garbizu, S., Arbelaiz, A., & Mondragon, I. (2004a). Stem and bunch banana fibers from cultivation wastes: Effect of treatments on physico-chemical behavior. *Journal of Applied Polymer Science, 94*(4), 1489–1495.

Gañán, P., Zuluaga, R., Cruz, J., Vélez, J., Retegí, A., & Mondragon, I. (2008). Elucidation of the fibrous structure of Musaceae maturate rachis. *Cellulose, 15*(1), 131–139.

Gañán, P., Zuluaga, R., Vélez, J., & Mondragon, I. (2004b). Biological natural retting for determining the hierarchical structuration of banana fibers. *Macromolecular Bioscience, 4*(10), 978–983.

Gritsch, C. S., Kleist, G., & Murphy, R. J. (2004). Developmental changes in cell wall structure of phloem fibres of the bamboo *Dendrocalamus asper*. *Annals of Botany, 94*(4), 497–505.

Habibi, Y., Heux, L., Mahrouz, M., & Vignon, M. R. (2008). Morphological and structural study of seed pericarp of *Opuntia Ficus-Indica* prickly pear fruits. *Carbohydrate Polymers, 72*(1), 102–112.

Hayashi, T., Marsden, M. P. F., & Delmer, D. P. (1987). Pea xyloglucan and cellulose. *Plant Physiology, 83*(2), 384–389.

Helbert, W., Sugiyama, J., Ishihara, M., & Yamanaka, S. (1997). Characterization of native crystalline cellulose in the cell walls of Oomycota. *Journal of Biotechnology, 57*(1–3), 29–37.

Higgins, H. G., Stewart, C. M., & Harrington, K. J. (1961). Infrared spectra of cellulose and related polysaccharides. *Journal of Polymer Science, 5*(1), 59–84.

Hindeleh, A. M. (1980). X-ray characterization of viscose rayon and the significance of crystallinity on tensile properties. *Textile Research Journal, 50*(10), 581–589.

Hubbe, M., Rojas, O., Lucia, L., & Sain, M. (2008). Cellulosic nanocomposites: A review. *BioResources, 3*(3), 929–980.

Isogai, A., Usuda, M., Kato, T., Urdu, T., & Atalla, R. H. (1989). Solid-state CP/MAS ^{13}C NMR study of cellulose polymorphs. *Macromolecules, 22*(7), 3168–3172.

Kacuráková, M., Capek, P., Sasinková, V., Wellner, N., & Ebringerová, A. (2000). FT-IR study of plant cell wall model compounds: Pectic polysaccharides and hemicelluloses. *Carbohydrate Polymers, 43*(2), 195–203.

Kataoka, Y., & Kondo, T. (1996). Changing cellulose crystalline-structure in forming wood cell-walls. *Macromolecules, 29*(19), 6356–6358.

Lai-Kee-Him, H., Chanzy, H., Müler, M., Putaux, J-L., Imai, T., & Bulone, V. (2002). In vitro versus in vivo cellulose microfibrils from plant primary wall synthases: Structural differences. *The Journal of Biological Chemistry, 277*(40), 36931–36939.

Liang, C. Y., & Marchessault, R. H. (1959). Infrared spectra of crystalline polysaccharides. I. Hydrogen bonds in native celluloses. *Journal of Polymer Science, 37*(132), 385–395.

Liu, C. F., Xu, F., Sun, J. X., Ren, J. L., Sun, R. C., Curling, S., et al. (2006). Physicochemical characterization of cellulose from perennial ryegrass leaves (*Lolium perenne*). *Carbohydrate Research, 341*(16), 2677–2687.

Malainine, M. E., Dufresne, A., Dupeyre, D., Mahrouz, M., Vuong, R., & Vignon, M. R. (2003). Structure and morphology of cladodes and spines of *Opuntia ficus-indica*. Cellulose extraction and characterization. *Carbohydrate Polymers, 51*(1), 77–83.

Morán, J. I., Alvarez, V. A., Cyras, V. P., & Vázquez, A. (2008). Extraction of cellulose and preparation of nanocellulose from sisal fibers. *Cellulose, 15*(1), 149–159.

Newman, H. R. (2008). Simulation of X-ray diffractograms relevant to the purported polymorphs cellulose IV_I and IV_{II}. *Cellulose*. doi:10.1007/s10570-008-9225-5.

Newman, R. H. (1997). Crystalline forms of cellulose in the silver tree fern *Cyathea dealbata*. *Cellulose, 4*(4), 269–279.

Nishiyama, Y., Kuga, S., & Okano, T. (2000). Mechanism of mercerization revealed by X-ray diffraction. *Journal of Wood Science, 46*(6), 452–457.

Okano, T., & Sarko, A. (1985). Mercerization of cellulose. II. Alkali-cellulose intermediates and a possible mercerization mechanism. *Journal of Applied Polymer Science, 30*(1), 325–332.

Renard, C. M. G. C., & Jarvis, M. C. (1999). A cross-polarization, magic-angle-spinning, ^{13}C-nuclear-magnetic-resonance study of polysaccharides in sugar beet cell walls. *Plant Physiology, 119*(4), 1315–1322.

Rondeau-Mouro, C., Bouchet, B., Pontoire, B., Robert, P., Mazoyer, J., & Buléon, A. (2003). Structural features and potential texturising properties of lemon and maize cellulose microfibrils. *Carbohydrate Polymers, 53*(3), 241–252.

Saito, T., Nishiyama, Y., Putaux, J-L., Vignon, M. R., & Isogai, A. (2006). Homogeneous suspensions of individualized microfibrils from TEMPO-catalyzed oxidation of native cellulose. *Biomacromolecules, 7*(6), 1687–1691.

Sao, K., Mathew, M. D., & Ray, P. K. (1987). Infrared spectra of alkali treated degummed Ramie. *Textile Research Journal, 57*(7), 407–414.

Satyanarayana, K. G., Pillai, C. K. S., Sukumaran, K., Rohatgi, P. K., & Vijayan, K. (1982). Structure property studies of fibres from various parts of the coconut tree. *Journal of Materials Science, 17*(8), 2453–2462.

Sugiyama, J., Vuong, R., & Chanzy, H. (1991). Electron diffraction study on the two crystalline phases occurring in native cellulose from an algal cell wall. *Macromolecules, 24*(14), 4168–4175.

Sun, J. X., Sun, X. F., Zhao, H., & Sun, R. C. (2004). Isolation and characterization of cellulose from sugarcane bagasse. *Polymer Degradation and Stability, 84*(2), 331–339.

Sun, R. C., Sung, X. F., Liu, G. Q., Fowler, P., & Tomkinson, J. (2002). Structural and physicochemical characterization of hemicelluloses isolated by alkaline peroxide from barley straw. *Polymer International, 51*(2), 117–124.

Sun, R. C., Tomkinson, J., Mao, F. C., & Sun, X. F. (2001). Physicochemical characterization of lignins from rice straw by hydrogen peroxide treatment. *Journal of Applied Polymer Science, 79*(4), 719–732.

Sun, X. F., Xu, F., Sun, R. C., Fowler, P., & Baird, M. S. (2005). Characteristics of degraded cellulose obtained from steam-exploded wheat straw. *Carbohydrate Research, 340*(1), 97–106.

Tilby, E. (1994). Method and apparatus for processing sugarcane. US Patent office, Pat. No. 3567511.

Turbak, A., Snyder, F., & Sandberg, K. (1983). Microfibrillated cellulose, a new cellulose product: Properties, uses, and commercial potential. *Journal of Applied Polymer Science. Applied Polymer Symposium, 37*, 815–827.

Wada, M., Heux, L., & Sugiyama, J. (2004). Polymorphism of cellulose I family: Reinvestigation of cellulose IV_I. *Biomacromolecules, 5*(4), 1385–1391.

Wada, M., Okano, T., Sugiyama, J., & Horii, F. (1995). Characterization of tension and normally lignified wood cellulose in *Populus maximowiczii*. *Cellulose, 2*(4), 223–233.

Wang, B., & Sain, M. (2007). Isolation of nanofibers from soybean source and their reinforcing capability on synthetic polymers. *Composites Science and Technology, 67*(11–12), 2517–2521.

Wang, B., Sain, M., & Oksman, K. (2007). Study of structural morphology of hemp fiber from the micro to the nanoscale. *Applied Composite Materials, 14*(2), 89–103.

Xiao, B., Sun, X. F., & Sun, R. C. (2001). Chemical, structural, and thermal characterizations of alkali-soluble lignins and hemicelluloses, and cellulose from maize stems, rye straw, and rice straw. *Polymer Degradation and Stability, 74*(2), 307–319.

Xu, F., Sun, J. X., Geng, Z. C., Liu, C. F., Ren, J. L., Sun, R. C., et al. (2007a). Comparative study of water-soluble and alkali-soluble hemicelluloses from perennial ryegrass leaves (*Lolium peree*). *Carbohydrate Polymers, 67*(1), 56–65.

Xu, F., Sun, J. X., Sun, R. C., Fowler, P., & Baird, M. S. (2006). Comparative study of organosolv lignins from wheat straw. *Industrial Crops and Products, 23*(2), 180–193.

Xu, F., Zhou, Q. A., Sun, J. X., Liu, C. F., Ren, J. L., Sun, R. C., et al. (2007b). Fractionation and characterization of chlorophyll and lignin from de-juiced Italian ryegrass

(*Lolium multifolrum*) and timothy grass (*Phleum pratense*). *Process Biochemistry, 42*(5), 913–918.

Yano, H., & Nakahara, S. (2004). Bio-composites produced from plant microfiber bundles with a nanometer unit web-like network. *Journal of Materials Science, 39*(5), 1635–1638.

Zhong, R., Burk, D. H., & Ye, Z. (2001). Fibers. A model for studying cell differentiation, cell elongation, and cell wall biosynthesis. *Plant Physiology, 126*(2), 477–479.

Zuluaga, R., Putaux, J-L., Restrepo, A., Mondragon, I., & Gañán, P. (2007). Cellulose microfibrils from banana farming residues: Isolation and characterization. *Cellulose, 14*(6), 585–592.